Intercellular Adhesion Molecule-1 Dimerization and Its Consequences for Adhesion Mediated by Lymphocyte Function Associated-1

By Jim Miller,* Ruth Knorr,* Marco Ferrone,* Roya Houdei,* Christopher P. Carron,‡ and Michael L. Dustin*

*From the *Center for Immunology and Department of Pathology, Washington University School of Medicine and the Department of Pathology, Jewish Hospital of St. Louis, St. Louis, Missouri 63110; and ‡Department of Immunology, Searle Research and Development, Monsanto Corporate Research, Chesterfield, Missouri 63110*

Summary

Intercellular adhesion molecule-1 (ICAM-1, CD54) is a ligand for the integrins lymphocyte function associated-1 (LFA-1, CD11a/CD18) and complement receptor-3 (Mac-1, CD11b/CD18) making it an important participant in many immune and inflammatory processes. Modified recombinant soluble ICAM-1 formed dimers. This result indicated that the ectodomain of ICAM-1 contains homophilic interaction sites. Soluble ICAM-1 dimers bind to solid-phase purified LFA-1 with high avidity (dissociation constant [K_d] = 8 nM) in contrast to soluble ICAM-1 monomers whose binding was not measurable. Cell surface ICAM-1 was found to be dimeric based on two distinct criteria. First, a monoclonal antibody specific for monomeric soluble ICAM-1, CA7, binds normal ICAM-1 poorly at the cell surface; this antibody, however, binds strongly to two mutant forms of ICAM-1 when expressed at the cell surface, thus identifying elements required for dimer formation. Second, chemical cross-linking of cell surface ICAM-1 on transfected cells and tumor necrosis factor–activated endothelial cells results in conversion of a portion of ICAM-1 to a covalent dimer. Cell surface ICAM-1 dimers are more potent ligands for LFA-1–dependent adhesion than ICAM-1 monomers. While many extracellular matrix-associated ligands of integrins are multimeric, this is the first evidence of specific, functionally important homodimerization of a cell surface integrin ligand.

Cell adhesion is a regulated process mediated by specific molecular interactions between adhesion receptors (1, 2). Regulated changes in adhesion are critical in morphogenesis, wound healing, the integrity of solid tissues, and host defense (3–5). Lymphocytes take advantage of an intersection between two adhesion molecule families, the integrin family and the Ig superfamily, to bring cell–cell adhesion under control of specific immunological recognition events (2). The lymphocyte integrin LFA-1 responds to lymphocyte activation by increasing its avidity for its three known ligands, intercellular adhesion molecules (ICAMs)[1]-1, -2, and -3, which are members of the Ig superfamily (2, 3).

While many extracellular matrix ligands for integrins are dimers or higher oligomers (6), little is known of the organization of cell surface adhesion molecules (7–9). Membrane proteins may oligomerize with substantial lateral contact between molecules (10, 11) or may exist as preformed clusters with local concentration but no evidence of direct interaction (7). Oligomerization or clustering both may favor adhesion by suppressing net dissociation (12). However, the specific subunit relationships in oligomeric receptors, but absent in clusters, may uniquely contribute to ligand-induced conformational changes and signaling events (13, 14).

ICAM-1 is the most potent ligand for adhesion mediated by binding of LFA-1 (15, 16). While it has been assumed that the potency of ICAM-1 as an LFA-1 ligand may be related to specific properties of its unitary interaction with LFA-1, it is also possible that the surface presentation of ICAM-1 may have a role in its effectiveness. Along these lines, ICAM-1 has been shown to cluster at one pole of activated T and B lymphocytes at light microscopy resolution (0.6 μm) (17–19). Cell surface resonance energy transfer with bivalent antibodies suggest that ICAM-1 may self-associate and associate with other surface molecules (20, 21). However, studies with soluble recombinant ICAM-1 have led to the conclusion that ICAM-1 is monomeric (22, 23).

[1] *Abbreviations used in this paper:* BCECF-AM, 2′,7′-bis-(2-carboxymethyl)-5-(and 6)-carboxyfluorescein, acetomethoxy ester; BS_3, bis (sulfosuccinimidyl) suberate; DSS, disuccinimidyl suberate; GPI, glycosylphosphatidyl inositol; HA, hemagglutinin; HUVEC, human umbilical vein endothelial cells; ICAM, intercellular adhesion molecule.

 J. Exp. Med. © The Rockefeller University Press • 0022-1007/95/11/1231/11 $2.00
Volume 182 November 1995 1231–1241

Here, mAbs to ICAM-1 and chemical cross-linking have been used to evaluate the hypothesis that ICAM-1 is oligomeric at the cell surface. These studies were initiated by the observation that subtle modifications of soluble recombinant ICAM-1 allowed it to form stable noncovalent dimers in solution. We conclude that ICAM-1 forms homodimers at the cell surface and that the transmembrane domain and domain 3 contribute to dimerization. Homodimers formed by transmembrane ICAM-1 support greater levels of LFA-1–dependent cell adhesion than the monomers formed by a chimeric glycolipid–anchored form of ICAM-1.

Materials and Methods

Reagents and Enzymes. Reagents were obtained from Sigma Chemical Co., St. Louis, MO, or Fisher Scientific Co., Pittsburgh, PA, unless otherwise indicated. FITC goat anti–mouse IgG (H+L) was acquired from Zymed Laboratories (South San Francisco, CA). Reagents for Western blotting and chemiluminescent detection of mouse and rabbit antibodies were purchased from Amersham Corp. (Arlington Heights, IL). Octyl-β-D-glucopyranoside and hygromycin B were purchased from Calbiochem Corp. (La Jolla, CA). Lipofectamine and Geneticin were purchased from GIBCO BRL (Gaithersburg, MD). 2′,7′-bis-(2-carboxymethyl)-5-(and 6)-carboxyfluorescein, acetomethoxy ester (BCECF-AM) and FITC were purchased from Molecular Probes, Inc. (Eugene, OR). Disuccinimidyl (DSS) and bis(sulfosuccinimidyl) suberate (BS_3) cross-linkers were purchased from Pierce Chemical Co. (Rockford, IL). Soluble recombinant ICAM-1 purified by nonaffinity and immunoaffinity methods was a gift of Steven D. Marlin, Boehringer Ingelheim Pharmaceuticals, Inc. (Ridgebury, CT). Antiserum reactive with the cytoplasmic tail of ICAM-1 was a gift of Takashi K. Kishimoto, Boehringer Ingelheim.

Cell Lines and Antibodies. The T lymphoma SKW3, the B lymphoblastoid cell line JY, the TS2/4 hybridoma were obtained from T. Springer (Center for Blood Research, Boston, MA). TS1/22, TS1/18, and TS2/18 hybridomas and COS 1 cells were from American Type Culture Collection, Rockville, MD. BHK VP16 cells were generated at Monsanto Chemical Co., St. Louis, MO. (24). Human umbilical vein endothelial cells (HUVEC) were purchased from Clonetics Corp. (San Diego, CA). HUVEC were treated with 10 ng/ml TNF (Collaborative Research, Lexington, MA) before use in flow microfluorimetry and cross-linking experiments. CL203 ascites was a gift of S. Ferrone (Upstate Medical College, Valhalla, NY). Purified NKI-L16 was a gift of C. Figdor (University Hospital, Nijmegen, The Netherlands). Purified RR1/1 was a gift of R. Rothlein (Boehringer Ingelheim Pharmaceuticals, Inc.). M174F5B7, M178A7A1, and M261PP5C7 were generated and characterized at Monsanto Chemical Co. (24). Affinity-purified rabbit anti–ICAM-1 ectodomain and a crude antiserum against the ICAM-1 cytoplasmic tail were prepared by injecting rabbits with soluble recombinant ICAM-1 (25).

DNA Constructs and Expression of Recombinant Proteins. BHK-VP16 cells expressing ICAM-1 with a hemagglutinin tag were grown in DME 10% FCS, 453 U/ml hygromycin, and 200 μg/ml of G418. Soluble ICAM-1 was produced in a cell factory (Nunc, Roskilde, Denmark) and purified by immunoaffinity chromatography on M174F5B7 Affigel with elution at pH 3.0 and immediate neutralization (24). Sequencing of ICAM-1-HA revealed an Arg to Trp conversion at residue 361 (R361W) in domain 4 which is probably a PCR artifact. This mutation does not affect interaction with LFA-1 but we cannot rule out that this change has a role in stable dimer formation. Plasmids encoding full-length transmembrane ICAM-1 (26), glycosylphosphatidyl inositol (GPI)-anchored ICAM-1 (27), and ICAM-1, with removal of domain 3, domain 5, or the cytoplasmic tail (22) in the vector CDM8, were obtained from T. Springer (Center for Blood Research). Constructs in CDM8 were transfected into COS cells by the DEAE-Dextran method (28) and analyzed between 24 and 72 h after transfection. The full-length ICAM-1 and GPI-anchored ICAM-1 cDNA were subcloned into the vector 3360B (24) and transfected into BHK-VP16 cells with lipofectamine to produce stable cell lines expressing high levels of transmembrane and GPI-anchored ICAM-1.

Protein Iodination. Soluble ICAM-1 was iodinated with 1,3,4,6-tetrachloro-3α,6α-diphenylglycouril (29). 30 μg of ICAM-1 was iodinated with 1 mCi of $Na^{125}I$ and separated from free iodine on Sephadex G-25. mAbs were similarly iodinated with 1 mCi/100 μg protein.

Solid-Phase Receptor Binding Assays. Immunoaffinity purified LFA-1 (18) was adsorbed to polystyrene as previously described (30). Briefly, LFA-1 in 1% octylglucoside detergent was diluted into 9 vol PBS/2 mM $MgCl_2$ in wells of an untreated microtiter plate (Nunc; Corning Glass Inc., Corning, NY; or ICN/Flow, Costa Mesa, CA) and incubated for 1 h at room temperature with gentle agitation (microplate shaker set at 4–5; Bellco Biotechnology, Vineland, NJ). The solution was aspirated and the plates were blocked with 1% heat-treated BSA in PBS/2 mM $MgCl_2$ plus 0.02% NaN_3. Heat-treated BSA solutions were prepared by bringing a 1% BSA solution in PBS/2 mM $MgCl_2$ to 80°C in a microwave oven followed by rapid cooling to room temperature and 0.2-μm filtration. After blocking with the heat treated BSA for at least 1 h at room temperature the plates were washed with PBS/2 mM $MgCl_2$ and stored in this solution until use. These plates were rinsed with assay buffer (PBS, pH 7.4, 5% fetal bovine serum, 2 mM $MgCl_2$, and 0.02% NaN_3) before adding iodinated ICAM-1 for the indicated time at 4°C. The plates were rapidly washed four times and the bound radioactivity was released with sequential 1 N NaOH and 1 N acetic acid washes that were pooled for gamma counting.

Immunoradiometric Assays. The capture antibody was adsorbed to Nunc Maxisorb plates (Nunc) at 25 μg/ml in PBS overnight. After blocking with heat-treated BSA as above the plates were washed with assay medium and the samples containing purified proteins were added and incubated for at least 1 h at 4°C. The plates were then washed three times with assay medium and the iodinated detection reagent was added in excess and incubated at least 1 h at 4°C. The plates were then washed four times with assay medium and the bound radioactivity was eluted with 1 N NaOH then 1 N acetic acid as above. If the sample contained membrane proteins then assay medium was substituted with 25 mM Tris, pH 8.0, 1% Triton X-100, 0.15 M NaCl, and the plates were blocked again with heat-treated BSA before addition of the iodinated detection antibody in assay media.

Gel Filtration and Sedimentation. Gel filtration was performed on a fast performance liquid chromatography system (Pharmacia LKB Biotechnology, Piscataway, NJ) using the indicated columns. Sedimentation through 5–20% sucrose gradients was used to determine the sedimentation coefficient by interpolation from standard proteins. Data from gel filtration, sedimentation, and the estimated partial specific volume were used to calculate molecular weights using the Svedberg equation: mol wt = $(6\pi\eta_{(20,w)}NaS_{(20,w)})/$

$(1-\upsilon\rho_{20,w})$, where η is the viscosity of water at 20°C, N is Avogadro's number, a is the Stoke's radius, $S_{20,w}$ is the sedimentation coefficient corrected to water at 20°C, υ is the partial specific volume, and $\rho_{20,w}$ is the density of water at 20°C (31, 32). The columns and sucrose gradients were calibrated for measurement of Stoke's radius and sedimentation coefficient using ovalbumin (43 kD, 2.76 nm, 3.5 S), BSA (66 kD, 3.70 nm, 4.5 S), aldolase (150 kD, 4.74 nm, 7.6 S), catalase (200 kD, 5.22 nm, 11.2 S), and ferritin (430 kD, 6.1 nm) (31, 33).

Flow Cytometry. Monodispersed suspension of adherent cells was obtained by treatment of cell layers with HBSS with no $CaCl_2$ or $MgCl_2$ and 0.5 mM EDTA. Suspension cells were taken from log phase cultures. The cells were washed with HBSS plus 5% FBS, 0.5 mM EDTA, 0.02% NaN_3 (staining media). 10^6 cells were incubated in 50 μl of staining medium plus the primary antibody for 60 min at 4°C and then washed two times. The secondary antibody was then added at 10 μg/ml in 50 μl of staining medium, incubated an additional 30 min at 4°C, and the cells were washed twice. The stained cells were analyzed within 12 h on a FACScan® (Becton Dickinson and Co., Mountain View, CA).

Chemical Cross-Linking. Soluble ICAM-1 was cross-linked at room temperature in PBS, pH 7.4, with the indicated concentrations of DSS dissolved in DMSO. The cross-linking was allowed to proceed for 30 min before addition of excess glycine. The samples were then subjected to reducing SDS-PAGE. Cell surface cross-linking was performed on ice with all reagents prechilled. In some experiments cells were first iodinated by the glucose–oxidase-coupled lactoperoxidase method using 1 mCi of $^{125}I/2 \times 10^7$ cells (34, 35). Cells (10^5–10^6) in 100 μl of cold PBS, pH 7.4, were treated with the indicated concentration of BS_3, dissolved immediately before use in 150 mM NaCl, 0.1 mM HCl at 100 mM, for 30 min followed by blocking with excess glycine and simultaneous treatment with 5 mM iodoacetamide for 10 min on ice to alkylate free sulfhydryl groups within the intact cells. The cells were then pelleted and resuspended in 0.5 ml of lysis buffer (25 mM Tris, pH 8.0, 1% Triton X-100, 0.15 M NaCl, 5 mM EDTA, 5 mM iodoacetamide, 1 mM PMSF, and 50 millitrypsin inhibitor units of aprotinin) and sonicated for 10 s at a setting of 1 with a microtip probe sonicator on ice (sonifier 450; Branson Ultrasonics Corp., Danbury, CT). The sonicate was centrifuged at 30,000 *g* for 15 min and the supernatant was processed by immunoprecipitation, SDS-PAGE, and autoradiography, or by SDS-PAGE and Western blotting.

Immunoprecipitation. The cleared lysate was incubated overnight at 4°C with 25 μl of irrelevant antibody Sepharose CL-4B to remove nonspecifically binding components. The supernatant was then incubated with 25 μl of specific antibody Sepharose CL-4B (a mixture of RR1/1, CL203, and M174 for ICAM-1) for 2 h at 4°C. After this incubation the supernatant was removed and the beads were washed extensively, heated to 100°C with SDS-PAGE sample buffer, and subjected to reducing SDS-PAGE. The gels were dried and subjected to film autoradiography with an intensifying screen.

Western Blotting. The cleared lysate was mixed with 50 μl of wheat germ agglutinin agarose (EY Laboratories, San Mateo, CA) for 1 h at 4°C, followed by washing of the resin twice with lysis buffer followed by one wash with 10 mM Tris, pH 7.5. The washed wheat germ agglutinin agarose was treated with nonreducing SDS-PAGE sample buffer (including 50 mM iodoacetamide) at 100°C for 5 min and the soluble fraction was subjected to SDS-8%-PAGE. The glycoproteins were electrophoretically transferred to nitrocellulose, blocked with 5% nonfat dry milk in PBS 0.1% Tween-20, and incubated with the indicated primary antibodies which were detected by secondary horseradish peroxidase antibodies and enhanced chemiluminescence on x-ray film.

Cell Adhesion Assays. JY cells were fluorescently labeled using a solution of 5 μM BCECF-AM in RPMI-1640 medium plus 2% fetal bovine serum for up to 2×10^7 cells in 5 ml. The cells were incubated with BCECF-AM for 45 min in a 37°C in a 5% CO_2 incubator with periodic agitation after which they were washed four times with assay medium (RPMI-1640 10% fetal bovine serum, 5 mM Hepes, pH 7.4). The cells to be used as targets were plated in 96-well plates at 5×10^3–10^4 cells/well and allowed to grow to 2–4 $\times$ 10^4 cell/well. The cell layers were washed twice with assay media before adding blocking antibodies at 10 μg/ml. 10^5 BCECF-labeled cells were added in 50 μl of assay medium and the plates were centrifuged 5 min at 10 *g* to bring the BCECF-labeled cells into contact with the monolayer. The plates were then read quickly on a microplate fluorimeter (Cytofluor 2300; Millipore, Marlborough, MA) to determine the fluorescence level from each well. This required ~1 min. The plates were then incubated for 15 min at 37°C by flotation in a 37°C water bath and then washed four times with prewarmed medium using a 12-channel vacuum manifold (Drummond Scientific Co., Broomall, PA) operating at 25 inches of Hg vacuum. Between washes medium was added down the sides of the wells with a 12- or 8-channel pipettor. The assay medium was replaced and the plates were read on the microplate fluorimeter. Percent cell binding was determined on a well-for-well basis as the [(final reading − media blank)/(prewash reading − media blank)] × 100. All points were determined in quadruplicate with averaging after determination of percentage of cells bound.

Results

Hemagglutinin-tagged ICAM-1 Forms Oligomers. Soluble recombinant ICAM-1 generated by introducing a stop codon before the beginning of the transmembrane domain remains monomeric in solution even when concentrated to >20 mg/ml (22, 23) (Fig. 1 *A*). We were surprised to find that addition of a commonly used influenza hemagglutinin-derived epitope tag to the COOH-terminus of truncated soluble ICAM-1 (ICAM-1-HA) led to the ability of a significant proportion of ICAM-1-HA to form stable oligomers when concentrated to 15 mg/ml as indicated by gel filtration and sedimentation. Gel filtration resolved ICAM-1-HA into two peaks with apparent Stoke's radii of 5.22 and 6.14 nm (Fig. 1 *A*). Unmodified soluble recombinant ICAM-1 had an apparent Stoke's radius of 5.16 nm. These two peaks were then individually subjected to velocity sedimentation on 5–20% sucrose gradients. The smaller species sedimented in a sucrose gradient at 3.7 S while the larger sedimented at 5.45 S (Fig. 1 *B*). ICAM-1-HA has a mass of 67 kD by mass spectroscopy (Carron, C. P., unpublished observation). The partial specific volume (0.72 ml/g) was estimated from a polypeptide molecular mass of 51 kD and carbohydrate mass of 16 kD and the Svedberg equation was used to determine molecular masses of 79 and 147 kD for the small and large species, respectively (31). The large Stoke's radii are consistent with a rod-like shape of ICAM-1 (22, 36). These data show that ICAM-1-HA forms stable dimers with no higher oligomers, suggesting a specific interaction.

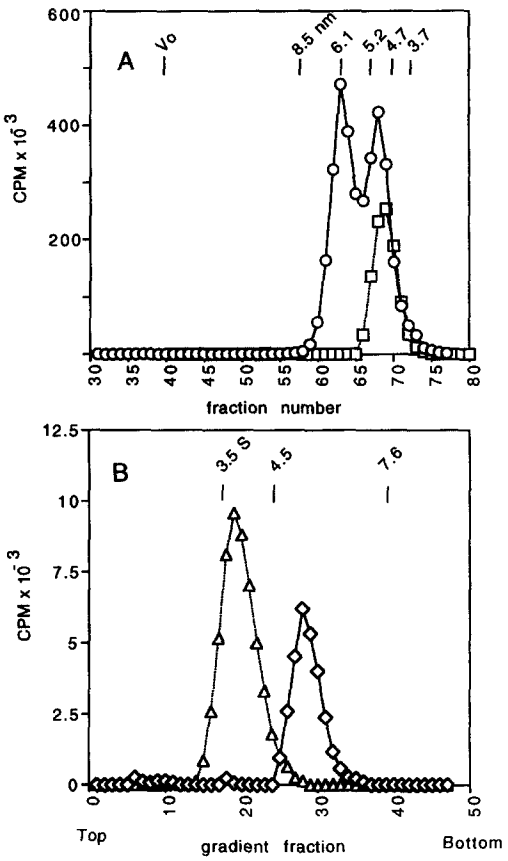

Figure 1. Dimerization of ICAM-1-HA. (*A*) sICAM-1 (*squares*) and ICAM-1-HA (*circles*) diluted from stocks of 22 and 15 mg/ml, respectively, were immediately iodinated and subjected to gel filtration on a 2.5 × 50-cm Superose 6 column run at 0.4 ml/min. 1-ml fractions were collected and analyzed for ^{125}I. All counts represented ICAM-1 based on ability to adsorb them to microtiter plate wells coated with CL203 (not shown). (*B*) Fraction 61 (*diamonds*) and 70 (*triangles*) from ICAM-1-HA gel filtration in *A* were sedimented on 5–20% sucrose gradients for 24 h at 38,000 rpm in an SW41 rotor (Beckman Instruments, Inc.). The gradients were fractionated from the top using a Gradifrac (Brinkmann Instruments, Inc.) and 48 fractions were collected into a microtiter plate. Standards were run in parallel.

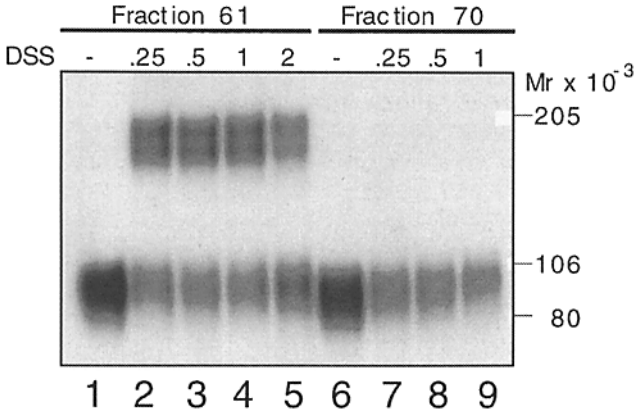

Figure 2. ICAM-1-HA dimers demonstrated by chemical cross-linking. Fractions 61 and 70 from Fig. 1 *A* were diluted in PBS and treated with DSS at the indicated millimolar concentration. After 30 min at room temperature the reaction was terminated by adding excess glycine and the samples were subjected to reducing SDS-6%-PAGE and autoradiography. The decrease in intensity of the fraction 70 bands with increasing cross-linker was not always observed and may be due to increased hydrophobicity of DSS-modified, nondimeric ICAM-1-HA.

Additional evidence for dimerization of ICAM-1-HA was obtained by chemical cross-linking. The small and large ICAM-1 species isolated by gel filtration were subjected to cross-linking with DSS and the results analyzed by reducing SDS-PAGE. Cross-linking over a range of DSS concentrations had no effect on migration of the ICAM-1-HA from fraction 70, but converted about half of ICAM-1-HA from fraction 61 to a doublet of 190 and 210 kD (Fig. 2). The two high molecular weight species are most likely representative of two cross-linking isomers of a single dimer. The doublet may result from formation of covalent bonds at two different points along the two ICAM-1 polypeptides. For example, one isomer may be cross-linked end to end, while the other may be cross-linked in the middle of the polypeptides to yield an X-shaped form that would migrate faster.

The HA tag itself has not been reported to induce dimerization of nonoligomeric proteins. A secreted molecule in which ICAM-1 domains 1 and 2 are followed by the same HA tag was monomeric at an even higher molar concentration than used to drive dimerization of the 5-domain ICAM-1-HA (data not shown). Thus it would appear that ICAM-1 domains 3–5 contain homophilic interaction sites that work in parallel with the HA-derived peptide sequence to form stable dimers. It is possible that the R361W mutation in domain 4 may contribute to the stability to the dimer. This mutation, however, is unlikely to have this effect unless there is a predisposition of ICAM-1 ectodomains to interact.

ICAM-1-HA Dimers Bind to Purified LFA-1 with High Avidity. Does ICAM-1 dimerization lead to an enhanced avidity for LFA-1? LFA-1 exists in at least two avidity states, low on resting lymphocytes and high on activated lymphocytes. However, even on activated cells, only a small fraction of LFA-1 molecules may be able to bind ICAM-1 (37). Immunoaffinity-purified LFA-1 provides a homogeneous source of high avidity LFA-1 (30). Iodinated ICAM-1-HA resolved into dimer- and monomer-enriched fractions by gel filtration (Fig. 1 *A*) was tested for binding to immunoaffinity-purified LFA-1 adsorbed to plastic. A peak of stable LFA-1 binding corresponding to the peak of ICAM-1-HA dimer was observed, while no binding was detected corresponding to the peak of ICAM-1-HA monomer. ICAM-1-HA dimer binding to immobilized LFA-1 displayed a two-component binding curve, suggesting a small number of high affinity binding sites that were saturated at the highest concentrations of ICAM-1-HA and a larger number of low affinity sites that were not saturated at the highest concentrations attainable in our experiments (Fig. 3 *B*). ICAM-1-HA dimer binding reached equilibrium after 1 h at 4°C with gentle agitation and displayed reversibility (not shown) suggesting that equilibrium binding

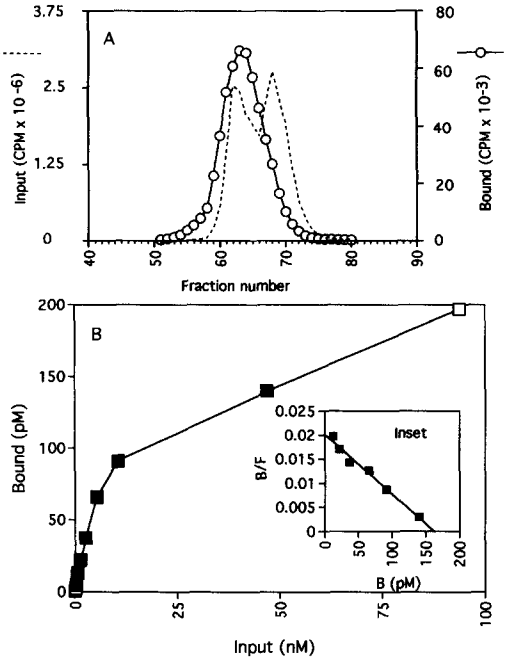

Figure 3. Binding of ICAM-1-HA dimers to immunoaffinity-purified LFA-1- A. ICAM-1-HA at 15 mg/ml was fractionated on a Superose 6 column as in Fig. 1 and the fractions were tested for binding to immunoaffinity-purified LFA-1 adsorbed to polystyrene by coincubation for 60 min at 4°C followed by four washes over a 2–3-min period. Remaining counts were determined (*solid line with circles*) and plotted against total counts (*dashed line*). (*B*) Dependence of ICAM-1-HA dimer binding to immunoaffinity-purified LFA-1 on ICAM-1-HA concentration. The data from the filled squares was replotted in the inset by the method of Scatchard (38) focusing on the high affinity class of binding sites for which near saturation is obtained.

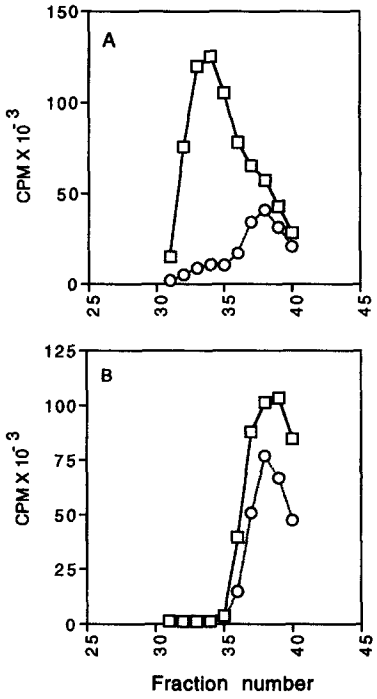

Figure 4. CA7 binds ICAM-1-HA monomer but not dimer. ICAM-1-HA 15 mg/ml (*A*) or sICAM-1 22 mg/ml (*B*) fractions from Superdex 200 column chromatography were tested for binding to immobilized CL203 (*squares*) or CA7 (*circles*). Binding of soluble ICAM-1 was detected with ^{125}I-RR1/1. The small amount of CA7 binding in dimer fraction is probably due to dissociation of dimers since the size of this peak increased progressively with storage of the column fractions (not shown).

analysis may be used to obtain an affinity. Scatchard analysis clearly demonstrated a high affinity component with a dissociation constant [K_d] of 8 nM (Fig. 3 *B*, *inset*). The maximum binding level for the high affinity sites corresponds to 10% of the LFA-1 sites detectable with iodinated antibodies to LFA-1 (not shown). This high affinity interaction suggests that dimeric ICAM-1 is functionally distinct from monomeric ICAM-1 and led us to examine cell surface ICAM-1 for oligomerization.

An mAb Selective for ICAM-1 Monomers Does Not Bind Cell Surface ICAM-1. The availability of the ICAM-1-HA dimers led us to test a panel of ICAM-1 mAbs for oligomerization-sensitive binding. Such an antibody could then be used to distinguish between ICAM-1 monomers and dimers at the cell surface. The mAb CA7 (Fig. 4, *circles*) bound monomeric ICAM-1 equally to our reference reagent CL203 (Fig. 4, *squares*) but bound dimeric ICAM-1-HA weakly. This monomer-specific antibody CA7 binds to the fifth Ig-like domain (23), whereas the other ICAM-1 mAbs, RR1/1, R6.5, and CL203 bind to domains 1, 2, and 4, respectively. Two other mAbs to domain 5, M178 and M261PP5C7, bound both monomeric and dimeric ICAM-1 HA similarly to CL203 (not shown).

We analyzed a number of cells expressing natural ICAM-1, including JY B lymphoblastoid cells (Fig. 5 *A* and Table 1), U937 premonocytic leukemia cells, three melanoma cell lines, and TNF-treated HUVEC (not shown), for binding of CA7 to ICAM-1 on live cells. We were surprised to find that the level of CA7 binding is <5–10% of binding of other ICAM-1 antibodies, including RR1/1 or CL203. In contrast, M261PP5C7 (Table 1) and M178 (not shown) bind ICAM-1 at the cell surface similarly to RR1/1 and CL203 (Table 1). Thus, most of the natural ICAM-1 at the cell surface appears dimeric based on CA7 binding.

Binding of CA7 to BHK cells expressing ICAM-1 mutants was tested to examine structural requirements for ICAM-1 dimerization. Replacement of ICAM-1s transmembrane and cytoplasmic tail through addition of a GPI anchor (27) resulted in binding of CA7 at a level similar to RR1/1 (Fig. 5 *C*; compare 5 *B*, Table 1). In contrast, ICAM-1 with all but two residues of the cytoplasmic tail deleted bound CA7 similarly to full-length ICAM-1, at <5% the level of RR1/1 (not shown). Together, these results implicate the transmembrane domain in ICAM-1 dimerization.

Deletion of domain 3 increased binding of CA7 relative to other ICAM-1 antibodies (Table 1). Therefore, high binding of CA7 can occur in a transmembrane-anchored form of ICAM-1 on live cells and domain 3 may also be involved in contacts leading to stabilization of ICAM-1 dimers.

Table 1. *Immunofluorescence Detection of ICAM-1 Epitopes*

Cell line	TS2/18	RR1/1	CL203	CA7	M261	Ratio CA7 ÷ RR1/1
JY	1.7	141	120	12	71	0.074
BHK ICAM-1.4	8.1	2,590	3,070	371	2,250	0.14
BHK GPI-ICAM-1.11	14.3	1,790	1,820	1,340	1,670	0.74
BHK ICAM-1 D3$^-$	8.0	359	83	217	177	0.59
BHK ICAM-1 D5$^-$	7.5	1,160	1,270	9.5	16	0.002

JY cells or stable BHK cell lines were stained with the indicated mAb at 10 ug/ml for 60 min at 4°C and then with 50 μg/ml FITC goat anti-mouse IgG. TS2/18 is an IgG1 mAb to human CD2 which is used as a negative control. Data are reported as the mean linear fluorescence in arbitrary but internally consistent units. The last column shows the ratio of specific CA7 staining to RR1/1 specific staining (TS2/18 background subtracted). Increasing primary antibody concentrations to 100 μg/ml and staining at 37°C for 30 min did not significantly increase CA7 staining relative to RR1/1. The staining pattern of JY cells for RR1/1 and CA7 is representative of staining of cell lines and primary cells that naturally express ICAM-1. A second new antibody to domain 5, M178A7A1, gave similar results to M261PP5C7.

ICAM-1 Cross-Linking at the Cell Surface Identifies ICAM-1 Dimers. Chemical cross-linking was used to analyze ICAM-1 neighbors on stably or transiently transfected cells. ICAM-1 epitopes are sensitive to chemical modification of lysines which are required for chemical cross-linking (Miller, J. M. and M. L. Dustin, unpublished observations) so a strategy was adopted in which covalent modifications were restricted to the ectodomain of ICAM-1 by using a non-membrane permeant cross-linker (BS_3) on intact cells, and an antibody to the cytoplasmic tail was then used to detect ICAM-1 on Western blots. Cross-linking was performed at 4°C since this has been shown to enhance specificity for cross-linking of oligomeric membrane proteins (39). To reduce nonspecific bands obtained with the anti-cytoplasmic tail antibody, glycoproteins were isolated on wheat germ agglutinin agarose before SDS-PAGE and Western blotting. In the absence of cross-linking, a diffuse 80–90-kD band typical of ICAM-1 on nonreduced gels was observed specifically in ICAM-1–transfected cells but not mock-transfected cells (Fig. 6). Addition of BS_3 at 4°C resulted in a shift of a portion of the immunoreactive 80–90-kD ICAM-1 to a 190-kD band (Fig. 6, and Fig. 7, lanes *4–6*). The proportion of ICAM-1 cross-linked under optimal conditions was ~20%. When similar experiments were performed with tran-siently transfected COS cells, virtually all of the 80–90-kD ICAM-1 shifted to 190 kD after cross-linking with 1 or 5 mM BS_3 (Fig. 7, lanes *1–3*). In both BHK cells and COS cells a single band was observed.

The hypothesis that ICAM-1 forms dimers at the cell surface was further tested in TNF-treated HUVEC which naturally express levels of ICAM-1 comparable to those in the ICAM-1–transfected BHK cells (Fig. 7, lanes *7–9*). The overall efficiency of ICAM-1 conversion to high molecular weight species in HUVEC was similar to that observed in BHK cells. However, in addition to the distinct band corresponding to dimeric ICAM-1, as observed in COS and BHK cells, a lower relative molecular mass band

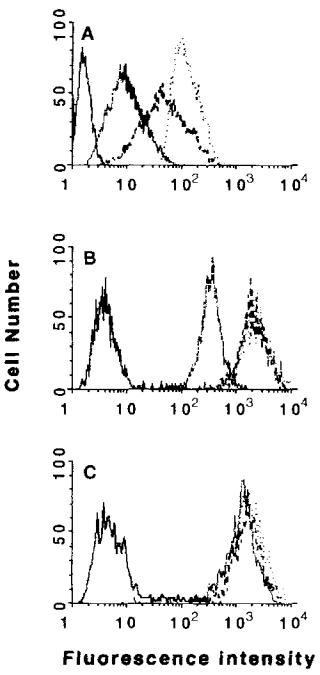

Figure 5. Differential ICAM-1 epitope expression on normal cells and ICAM-1 transfected cells. Binding of mouse mAbs TS2/18 (negative control, *solid*) RR1/1 (*dotted*), CA7 (*stippled*), and M261PP5C7 (*dashed*) was determined by subsequent binding of FITC goat anti-mouse IgG and flow microfluorimetry on a FACScan® (Becton Dickinson and Co.). Cells tested were (*A*) JY B lymphoblasts; (*B*) BHK-VP16 cells transfected with transmembrane ICAM-1; and (*C*) BHK-VP16 cells transfected with GPI-ICAM-1.

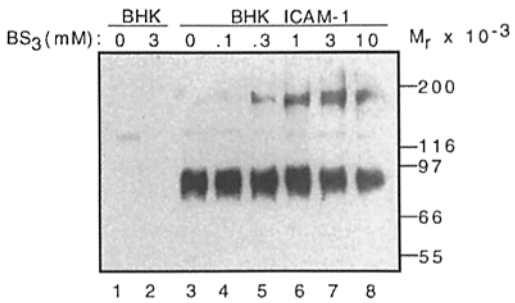

Figure 6. Chemical cross-linking of ICAM-1 at the surface of BHK (-VP16) and BHK-(VP16-)ICAM-1. Cells were incubated with the indicated concentration of BS_3 at 4°C and processed for nonreducing SDS-8%-PAGE as described in Materials and Methods. ICAM-1 was detected with an antibody to the cytoplasmic tail.

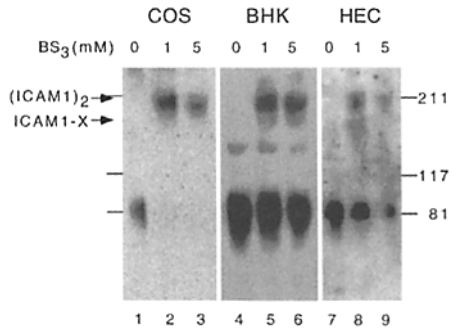

Figure 7. Chemical cross-linking of ICAM-1 at the surface of COS cells (lanes *1–3*), BHK cells (lanes *4–6*), and TNF-treated HUVEC (lanes *7–9*). HUVEC were treated with 10 ng/ml TNF for 24 h. ICAM-1 was detected with anti–cytoplasmic tail antiserum after cross-linking at the cell surface with the indicated concentration of BS_3 at 4°C.

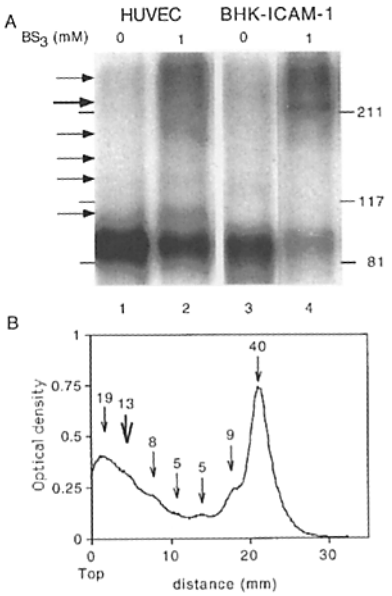

Figure 8. Chemical cross-linking of ICAM-1 at the surface of iodinated HUVEC and BHK cells. HUVEC were treated with 10 ng/ml TNF for 24 h. TNF-treated HUVEC and BHK cells were released from plates with HBSS/EDTA. Surface iodination and cross-linking were performed sequentially as rapidly as possible with cross-linking performed on ice. Immunoprecipitation was performed with a cocktail of ICAM-1 antibodies and the immunoprecipitates were run on SDS-8%-PAGE. (*A*) HUVEC (lanes *1* and *2*) or normal ICAM-1–transfected BHK cells (lanes *3* and *4*) without (lanes *1* and *3*) and with (lanes *2* and *4*) 1 mM BS_3. (*B*) Densitometry (personal densitometer; Molecular Dynamics, Sunnyvale, CA) on lane *2* with arrows pointing to bands and percentage of total optical density in the region under each band indicated.

corresponding to about one-third of the high molecular weight ICAM-1 was also detected in HUVEC.

The possibility that ICAM-1 may form heterodimers on the surface of endothelial cells was further evaluated by surface iodination, cross-linking, and immunoprecipitation with a cocktail of anti–ICAM-1 mAbs. A different pattern was obtained with TNF-treated HUVEC or BHK cells expressing transmembrane ICAM-1 (Fig. 8). After cross-linking with an optimal concentration of BS_3, the most prominent bands on reducing SDS-8%-PAGE of iodinated proteins immunoprecipitated from ICAM-1–transfected BHK cells are the 90-kD monomer, the 220-kD dimer, and a higher molecular weight smear that may represent higher order oligomers formed due to ICAM-1 clustering. ICAM-1 immunoprecipitated from cross-linked, TNF-treated HUVEC was distributed between several fainter bands, including the 220-kD dimer band and higher weight smear, but also including bands of 186, 160, 130, and a prominent band of 106 kD. The 186-kD band appears to correspond to the additional band in Fig. 7, lanes *8* and *9*. All of the additional bands were confirmed to contain ICAM-1 by Western blotting with anti–ICAM-1 ectodomain antibodies which are more sensitive than the anti–cytoplasmic tail antibodies (not shown). These results confirm that ICAM-1 homodimers exist on cells naturally expressing ICAM-1 and suggest that ICAM-1 heterodimers exist on endothelial cells. It is unlikely that these additional bands arise by proteolysis or nonspecific cross-linking to transiently encountered glycoproteins since the same methods applied to BHK and COS cells show predominantly only the monomeric and homodimeric ICAM-1 species.

When the cross-linking results are considered together with the observation that ICAM-1-HA forms dimers and that expression of a monomer-selective epitope on transmembrane ICAM-1 is low at the cell surface, the evidence that ICAM-1 can form dimers at the cell surface is compelling. On a cell naturally expressing ICAM-1, ICAM-1 exists primarily as a homodimer but may also form heterodimers with other molecules based on the appearance of a distinct cross-linked band.

Role of ICAM-1 Dimer in Cell Adhesion. It has been shown that GPI-ICAM-1–transfected COS cells adhere efficiently to surfaces coated with immunoaffinity-purified LFA-1 but no reports of lymphocyte adhesion to cells expressing GPI-ICAM-1 have been published. Transmembrane ICAM-1 is dimeric based on several criteria, while GPI-ICAM-1 is monomer-like, based on CA7 epitope expression. The effect of ICAM-1 dimerization on LFA-1–dependent cell adhesion was tested by examining adhesion of JY B lymphoblastoid cells to BHK cells stably expressing ICAM-1 or GPI-ICAM-1 at similar levels (Table 2). The expression levels were similar by flow cytometry after staining with RR1/1 and by radiometric assays with RR1/1 or CL203. JY cells were used because they are relatively deficient in β1 integrin family adhesion receptor activity which might increase the background binding to fibroblastoid cells (40, 41). JY cells showed twofold greater adhesion to the ICAM-1 than to GPI-ICAM-1 stably expressed at the same level in BHK cells and this pattern was retained when the JY cells were activated with NKI-L16 at 5 μg/ml (42). The adhesion was inhibited by LFA-1 mAb (Table 2). Thus, the dimeric presentation of transmembrane ICAM-1 is more effective in mediating LFA-1–dependent adhesion than the monomer-like presentation of GPI-ICAM-1.

Table 2. *JY Cell Adhesion to BHK Cells Expressing Different ICAM-1 forms*

Antibody	BHK-VP16	BHK-VP16-ICAM-1	BHK-VP16-GPI-ICAM-1	Δ
TS2/18	6.8 ± 1.4	21.2 ± 1.9 (14.4)	12.6 ± 1.7 (5.8)	2.1
TS1/22	4.2 ± 0.7	2.3 ± 0.6 (−1.9)	2.2 ± 0.8 (−2.0)	—
NKI-L16	7.9 ± 2.0	39.6 ± 6.5 (31.7)	26.1 ± 4.1 (18.2)	1.7

Data are based on a single experiment in which JY cells were incubated with BHK cell monolayers for 15 min at 37°C then washed with warm media. Specific adhesion is obtained by subtracting adhesion to the mock-transfected BHK cells from the adhesion to ICAM-1–transfected BHK cells and is shown in parentheses. The fold difference between the BHK-VP16-ICAM-1 and BHK-VP16-GPI-ICAM-1 was calculated by taking the specific binding in the presence of TS2/18 or NKI-L16 and subtracting the specific binding in the presence of TS1/22 and taking the ratio of these numbers for the two BHK cell types which are reported in the column "Δ." The experiment is representative of four other experiments performed with the same conditions.

Discussion

ICAM-1 is the most potent ligand for LFA-1 (15, 21, 26). The molecular basis of the greater avidity of LFA-1 for ICAM-1 compared with ICAM-2 or ICAM-3 has been a matter of speculation since it has not been possible to directly measure ICAM interaction with LFA-1 except through highly multivalent adhesive interactions. We have found that ICAM-1 forms homodimers at the cell surface and have investigated the impact of dimer formation on adhesion. Soluble ICAM-1 dimers bind stably to purified LFA-1, a property not previously observed with other forms of ICAM-1, suggesting that the dimers have an advantage in binding to LFA-1. Increased binding of soluble ICAM-1 dimers is also reflected in greater adhesion of lymphoblasts to cells expressing ICAM-1 dimers rather than ICAM-1 monomers. Greater activity of ICAM-1 dimers in cell adhesion may result from suppression of dissociation (43) or by more effective triggering of ligand induced conformational changes (13, 44). ICAM-2 does not cross-link with BS_3 suggesting that one of the reasons that ICAM-2 is a less potent ligand for LFA-1 than ICAM-1 is that it is monomeric while ICAM-1 is dimeric at the cell surface (Dustin, M. L., unpublished observations). ICAM-3 is very similar in overall structure to ICAM-1 so it will be of interest to evaluate whether it can form homodimers. Endothelial cells appear to express ICAM-1 heterodimers in parallel with homodimers, however, establishing the significance of this finding will require the generation of reagents to purify these putative heterodimers and assess their function relative to ICAM-1 homodimers and monomers. The most important contribution of the current studies is the demonstration that ICAM-1 forms homodimers at the cell surface and that these homodimers are more potent than monomer-like ICAM-1 forms generated by glycolipid anchoring.

An important tool in this study was an oligomerization-sensitive antibody, CA7, which recognizes an epitope in domain 5 of ICAM-1. CA7 was expressed on soluble monomeric ICAM-1 but not dimeric soluble ICAM-1 demonstrating that it is monomer selective. The CA7 epitope is weakly expressed on cells expressing normal transmembrane ICAM-1 compared with other ICAM-1 antibodies, suggesting that normal cell surface ICAM-1 is similar to the ICAM-1-HA homodimer. Interestingly, CA7 was strongly expressed on a glycolipid-anchored form of ICAM-1 and a domain 3–deleted form of transmembrane ICAM-1, suggesting that these molecules are similar to soluble ICAM-1-HA monomer. Not all domain 5 antibodies have this property of being monomer selective, suggesting that CA7 recognizes a unique epitope. CA7 expression is similarly low on all cells expressing transmembrane ICAM-1. The CA7 epitope is likely to recognize a region involved in ICAM-1 dimer contacts or surfaces made sterically inaccessible by dimer formation.

We have taken the first steps toward characterizing the structural basis of ICAM-1 dimerization and have targeted the transmembrane domain and domains 3–5 for further study. Transmembrane domains play a critical role in oligomerization of many membrane proteins, including glycophorin, the neu oncogene, and the T cell antigen–receptor complex (45–47). It is possible that the hemagglutinin tag with its alternating hydrophobic and hydrophilic residues effectively replaces the transmembrane domain of ICAM-1 in organizing formation of dimers by soluble ICAM-1-HA. The combined binding energies of the ectodomain interactions mediating ICAM-1 dimerization appear to be low based on the failure of conventional soluble ICAM-1 to form dimers. ICAM-1 domain 3 appears to contain a potential dimer contact region based on partial restoration of CA7 binding in domain 3 deletion mutants of ICAM-1. Domain 3 contains a hydrophobic region that is a good candidate for a homophilic contact site in ICAM-1 dimers. The failure of ICAM-1 domains 1 and 2 plus an HA tag to form dimers suggests that these domains do not contain significant sites of interaction in dimer formation. However, it is intriguing that a crystal structure of domains 1 and 2 of the related Ig superfamily member vascular cell adhesion molecule (VCAM)-1 shows a homodimeric unit cell (48).

The efficiency of ICAM-1 cross-linking differed among BHK cells stably expressing human ICAM-1, COS cells transiently expressing ICAM-1, and HUVEC that naturally express high levels of ICAM-1 in response to TNF treatment (40). In contrast, CA7 binding does not indicate a large difference in the level of ICAM-1 oligomerization among these cell types. It should be noted that even in

cases where 100% of molecules are in dimers it is not always possible to covalently cross-link all pairs due to competing processes that consume reactive lysines before intermolecular bridges are formed. However, the differences between ICAM-1 on different cells suggest that there are basic differences in the presentation of ICAM-1 or its conformation at the surface between these cell types. The difference in cross-linking efficiency may reflect a difference in access of the cross-linking reagent to ICAM-1. Some cells retain ICAM-1 in intracellular compartments (17) and it is possible that not all of the ICAM-1 detected by Western blotting in a specific cell type is at the surface. Furthermore, HUVEC display several ICAM-1 forms, suggesting the possibility of ICAM-1 heterodimers with unknown polypeptides that may themselves cross-link with different efficiencies.

ICAM-1 interacts with the cytoskeleton through its cytoplasmic tail but no evidence for a role of cytoskeletal binding in ICAM-1 dimerization was found. An ICAM-1 cytoplasmic tail deletion mutant was still dimeric based on lack of CA7 expression. The cytoplasmic tail of ICAM-1 binds α-actinin (49). Since α-actinin is dimeric it may promote ICAM-1 dimerization (12). Conversely, the binding of α-actinin to ICAM-1 cytoplasmic tails is weak at physiological ionic strength and may require ICAM-1 dimerization to allow bivalent binding (49). Thus, ICAM-1 dimerization may be important for ICAM-1 interactions on both faces of the plasma membrane.

ICAM-1 oligomerization at the cell surface has been suggested in other studies. ICAM-1 has been found to cluster in uropod structures in T and B lymphoblasts (17–19). This phenomenon is related to cytoskeletal association (19) and is probably a higher level of organization than the ICAM-1 dimers described here. A more recent study used fluorescence resonance energy transfer with bivalent antibodies labeled with green and red dyes (21). Those authors interpreted their data to suggest that ICAM-1 is dimeric on some cells and not on others, but we feel that the use of bivalent antibodies in these experiments limits their resolution to detecting clustering rather than molecular dimerization which would require monovalent probes. ICAM-1 has also been suggested to associate with the multisubunit IL-2 receptor by resonance energy transfer, however, it is unclear whether this represents association of ICAM-1 dimers with the IL-2 receptor or an ICAM-1 monomer forming a heterooligomer with the IL-2 receptor complex rather than another ICAM-1 monomer (20).

ICAM-1 is also a ligand for the neutrophil/macrophage integrin Mac-1 (CD11b/CD18). It will be important to determine the consequences of ICAM-1 dimerization for Mac-1 binding. LFA-1 binds to domains 1 and 2 of ICAM-1 while Mac-1 binds to domain 3 of ICAM-1. Domain 3 was implicated in dimerization in this study so we tested a number of domain 3 mutants affecting ICAM-1 binding to Mac-1 (D229QR/HLE, R231/I, N240DS/KNA, E254DE/KEK, N269/D) (50) for effects on CA7 epitope expression and did not find any change, suggesting that these mutants alter interaction of ICAM-1 and Mac-1 without affecting ICAM-1 dimerization (Knorr, R., and M. L. Dustin, unpublished observation).

Clustering of LFA-1 on activated lymphocytes has been suggested as a prerequisite for LFA-1–mediated adhesion (42). Resting lymphocytes appear to lack preclustered LFA-1 and therefore it has been suggested that they are not competent for LFA-1–mediated adhesion even when acutely activated (51). However, it is clear that T cell receptor cross-linking can induce a dramatic increase in LFA-1–dependent T cell adhesion to surfaces bearing purified ICAM-1 within minutes (30). We have found that purified ICAM-1 forms clusters upon reconstitution and this clustering, possibly mimicking cell surface dimerization, may be a critical element in our ability to demonstrate adhesion of acutely activating resting T cells to ICAM-1 substrates. Soluble recombinant ICAM-1 may not adequately mimic cell surface dimers when adsorbed to plastic in a monomeric form and this may account for the failure of some investigators to demonstrate rapid activation of LFA-1 on resting T cells for binding to ICAM-1 (51). Therefore, ICAM-1 homodimers may be the only suitable LFA-1 ligand for acutely activated resting T lymphocytes.

The evidence that ICAM-1 is dimeric at the cell surface and that this dimerization leads to enhanced binding of purified LFA-1 and cell adhesion is timely in that parallel studies have demonstrated three distinct ICAM-1–binding sites in LFA-1, two in the αL subunit, and one in the β2 subunit. All of these putative binding sites appear to include divalent cation-binding motifs (52–55) and may mediate coordination of a critical oxygenated residue(s) in ICAM-1 with metal ions held by two metal ion–dependent adhesion site motifs in LFA-1, one in αL and one in β2, and one EF hand-like structure in αL. ICAM binding to LFA-1 may then involve convergence of these metal ion positioning motifs onto one ICAM or binding to two or three different ICAM molecules. In the latter case the dimerization of ICAM-1 would offer a distinct advantage in optimally positioning two ICAM-1 molecules for LFA-1 binding and may account for the advantage of dimeric ICAM-1 in initiating LFA-1–dependent adhesion.

We thank Drs. E. Unanue and S. Teitelbaum for their generous support. M. L. Dustin thanks B. J. Bormann for sharing results before publication. We thank Drs. T. Springer, C. Figdor, T. Warren, P. Hippenmeyer, S. Ferrone, T. K. Kishimoto, S. Marlin, R. Rothlein, and S. Kornfeld for reagents and advice.

This work was supported in part by a grant from the Monsanto-Searle/Washington University Biomedical Program. A portion of this work had been published in abstract form (Dustin, M. L., C. Carron, B. J. Bor-

mann, M. Ferrone, J. Miller, and R. Houdei. 1994. *Mol. Biol. Cell.* 5:184a.).

Address correspondence to Michael L. Dustin, Washington University School of Medicine, Department of Pathology, Box 8118, St. Louis, MO 63110.

Note Added in Proof: While this paper was under review, another paper was published concluding that cell surface ICAM-1 is dimeric (Reilly, P. L., J. R. Woska, D. D. Jeanfavre, E. McNally, R. Rothlein, and B. J. Bormann. 1995. *J. Immunol.* 155:529–532.

Received for publication 10 April 1995 and in revised form 26 June 1995.

References

1. Edelman, G.M. 1986. Cell adhesion molecules in the regulation of animal form and tissue pattern. *Annu. Rev. Cell Biol.* 2:81–116.
2. Springer, T.A. 1994. Traffic signals for lymphocyte recirculation and leukocyte emigration: the multistep paradigm. *Cell.* 76:301–314.
3. Hynes, R.O. 1992. Integrins: versatility, modulation, and signalling in cell adhesion. *Cell.* 69:11–25.
4. McClay, D.R., and C.A. Ettensohn. 1987. Cell adhesion in morphogenesis. *Annu. Rev. Cell Biol.* 3:319–345.
5. Wessendorf, L.H.V., M. Wehrli, A. DiAntonio, and M. Wilcox. 1992. Genetic interactions with integrins during wing morphogenesis in Drosophila. *Cold Spring Harbor Symp. Quant. Biol.* 62:241–248.
6. Ayad, S., R.P. Boot-Handford, M.J. Humphries, K.E. Kadler, and C.A. Shuttleworth. 1994. The extracellular matrix facts book. Academic Press, Inc., San Diego, CA. 1–163.
7. Detmers, P.A., S.D. Wright, E. Olsen, B. Kimball, and Z.A. Cohn. 1987. Aggregation of complement receptors on human neutrophils in the absence of ligand. *J. Cell Biol.* 105: 1137–1145.
8. Horstkorte, R., M. Schachner, J.P. Magyar, T. Vorherr, and B. Schmitz. 1993. The fourth immunoglobulin-like domain of NCAM contains a carbohydrate recognition domain for oligomannosidic glycans implicated in association with L1 and neurite outgrowth. *J. Cell Biol.* 121:1409–1421.
9. Berlin, C., R.F. Bargatze, J. J. Campbell, U.H. von Andrian, .C. Szabo, S.R. Hasslen, R.D. Nelson, E.L. Berg, S.L. Erlandsen, and E.C. Butcher. 1995. Alpha4 integrins mediate lymphocyte attachment and rolling under physiological flow. *Cell.* 80:413–422.
10. Roth, M., A. Lewit-Bentley, H. Michel, J. Deisenhofer, R. Huber, and D. Oesterheit. 1989. Detergent structure in crystals of a bacterial photosynthetic reaction centre. *Nature (Lond.).* 340:659–662.
11. Wilson, I.A., J.J. Skehel, and D.C. Wiley. 1981. Structure of the haemagglutinin membrane glycoprotein of influenza virus at 3 A resolution. *Nature (Lond.).* 289:366–373.
12. Posner, R.G., B. Lee, D.H. Conrad, D. Holowka, B. Baird, and B. Goldstein. 1992. Aggregation of IgE-receptor complexex on rat basophilic leukemia cells does not change the intrinsic affinity but can alter the kinetics of the ligand-IgE interaction. *Biochemistry.* 31:5350–5356.
13. Du, X., E.F. Plow, A.L. Frelinger, T.E. O'Toole, J.C. Loftus, and M.H. Ginsberg. 1991. Ligands "activate" integrin alpha-IIb beta3 (platelet gpIIbIIIa). *Cell.* 65:409–416.
14. Clarke, E.A., M. Trikha, F.S. Markland, and J.S. Brugge. 1994. Structurally distinct disintegrins contortrostatin and multiaqamatin differentially regulate platelet tyrosine phosphorylation. *J. Biol. Chem.* 269:21940–21943.
15. de Fougerolles, A.R., X. Qin, and T.A. Springer. 1994. Characterization of the function of intercellular adhesion molecule (ICAM)-3 and comparison with ICAM-1 and ICAM-2 in immune responses. *J. Exp. Med.* 179:619–629.
16. Binnerts, M.E., Y. van Kooyk, D.L. Simmons, and C.G. Figdor. 1994. Distinct binding of T lymphocytes to ICAM-1, -2 or -3 upon activation of LFA-1. *Eur. J. Immunol.* 24:2155–2160.
17. Dougherty, G.J., S. Murdoch, and N. Hogg. 1988. The function of human intercellular adhesion molecule-1 (ICAM-1) in the generation of an immune response. *Eur. J. Immunol.* 18:35–39.
18. Dustin, M.L., O. Carpén, and T.A. Springer. 1992. Regulation of locomotion and cell–cell contact area by the LFA-1 and ICAM-1 adhesion receptors. *J. Immunol.* 148:2654–2663.
19. Carpén, O., D.E. Staunton, and T.A. Springer. 1992. Association of intercellular adhesion molecule-1 (ICAM-1) with actin-containing cytoskeleton and α-actinin. *J. Cell Biol.* 118: 1223–1234.
20. Burton, J., C.K. Goldman, P. Rao, M. Moos, and T.A. Waldmann. 1990. Association of intercellular adhesion molecule 1 with the multichain high-affinity interleukin 2 receptor. *Proc. Natl. Acad. Sci. USA.* 87:7329–7333.
21. Bene, L., M. Balázs, J. Matkó, J. Möst, M.P. Dieich, J. Szöllösi, and S. Damjanovch. 1994. Lateral organization of the ICAM-1 molecule at the surface of human lymphoblasts: a possible model for its codistribution with the IL-2 receptor, class I and class II HLA molecules. *Eur. J. Immunol.* 24:2115–2123.
22. Staunton, D.E., M.L. Dustin, H.P. Erickson, and T.A. Springer. 1990. The arrangement of the immunoglobulin-like domains of ICAM-1 and the binding sites for LFA-1 and rhinovirus. *Cell.* 61:243–254.
23. Rothlein, R., E.A. Mainolfi, M. Czajkowski, and S.D. Marlin. 1991. A form of circulating ICAM-1 in human serum. *J. Immunol.* 147:3788–3793.
24. Warren, T.G., P.J. Hippenmeyer, D.M. Meyer, B.A. Reitz, E. Rowold, and C.P. Carron. 1994. High-level expression of biologically active, soluble forms of ICAM-1 in a novel mammalian-cell expression system. *Protein Expr. Purif.* 5:498–508.
25. Marlin, S.D., D.E. Staunton, T.A. Springer, C. Stratowa, W. Sommergruber, and V. Merluzzi. 1990. A soluble form of intercellular adhesion molecule-1 inhibits rhinovirus infection. *Nature (Lond.).* 344:70–72.
26. Staunton, D.E., M.L. Dustin, and T.A. Springer. 1989. Functional cloning of ICAM-2, a cell adhesion ligand for LFA-1 homologous to ICAM-1. *Nature (Lond.).* 339:61–64.

27. Staunton, D.E., A. Gaur, P.Y. Chan, and T.A. Springer. 1992. Internalization of a major group human rhinovirus does not require cytoplasmic or transmembrane domains of ICAM-1. *J. Immunol.* 148:3271–3274.
28. Aruffo, A., and B. Seed. 1987. Molecular cloning of a CD28 cDNA by a high efficiency COS cell expression system. *Proc. Natl. Acad. Sci. USA.* 84:8573–8577.
29. Fraker, P.J., and J.C. Speck. 1978. Protein and cell membrane iodinations with a sparingly soluble chloroamide, 1,3,4,6-tetrachloro-3,6-diphenyl glycoluril. *Biochem. Biophys. Res. Commun.* 80:849–857.
30. Dustin, M.L., and T.A. Springer. 1989. T cell receptor cross-linking transiently stimulates adhesiveness through LFA-1. *Nature (Lond.).* 341:619–624.
31. Clarke, S. 1975. The size and detergent binding of membrane proteins. *J. Biol. Chem.* 250:5459–5469.
32. Sadler, J.E., J.I. Rearick, J.C. Paulson, and R.L. Hill. 1979. Purification to homogeneity of a beta-galactoside alpha2 to 3 sialyltransferase and partial purification of an alpha-*N*-acetylgalactosamine alpha2 to 6 sialyltransferase from porcine submaxillary glands. *J. Biol. Chem. 254*:4434–4443.
33. Terhorst, C., K. LeClair, A. Ma, and H. Slayter. 1981. Protein micelles of human histocompatibility antigens (HLA-A and HLA-B). *Mol. Immunol.* 18:103–112.
34. Hubbard, A.L., and Z.A. Cohn. 1972. The enzymatic iodination of the red cell membrane. *J. Cell Biol.* 55:390–405.
35. Trowbridge, I.S., and R. Hyman. 1975. Thy-1 variants of mouse lymphomas: biochemical characterization of genetic defect. *Cell.* 6:279–287.
36. Kirchhausen, T., D.E. Staunton, and T.A. Springer. 1995. Location of the domains of ICAM-1 by immunolabeling and single-molecule electron microscopy. *J. Leukocyte Biol.* 53: 342–346.
37. Diamond, M.S., and T.A. Springer. 1993. A subpopulation of Mac-1 (CD11b/CD18) molecules mediates neutrophil adhesion to ICAM-1 and fibrinogen. *J. Cell Biol.* 120:545–556.
38. Scatchard, G. 1949. The attractions of proteins for small molecules and ions. *Ann. NY Acad. Sci.* 51:660–672.
39. Fanger, B.O., K.S. Austin, H.S. Earp, and J.A. Cidlowski. 1986. Cross-linking of epidermal growth factor receptors in intact cells: detection of initial stages of receptor clustering and determination of molecular weight of high-affinity receptors. *Biochemistry.* 25:6414–6420.
40. Dustin, M.L., and T.A. Springer. 1988. Lymphocyte function–associated antigen-1 (LFA-1) interaction with intercellular adhesion molecule-1 (ICAM-1) is one of at least three mechanisms for lymphocyte adhesion to cultured endothelial cells. *J. Cell Biol.* 107:321–331.
41. Elices, M.J., L. Osborn, Y. Takada, C. Crouse, S. Luhowskyj, M.E. Hemler, and R.R. Lobb. 1990. VCAM-1 on activated endothelium interacts with the leukocyte integrin VLA-4 at a site distinct from the VLA-4/fibronectin binding site. *Cell.* 60:577–584.
42. van Kooyk, Y., P. Weder, F. Hogervorst, A.J. Verhoeven, G. van Seventer, A.A. te Velde, J. Borst, G.D. Keizer, and C.G. Figdor. 1993. Activation of LFA-1 through a Ca^{2+}-dependent epitope stimulates lymphocyte adhesion. *J. Cell Biol.* 112:345–354.
43. van der Merwe, P.A., A.N. Barclay, D.W. Mason, E.A. Davies, B.P. Morgan, M. Tone, A.K.C. Krishnam, C. Ianelli, and S.J. Davis. 1994. Human cell-adhesion molecule CD2 binds CD58 (LFA-3) with a very low affinity and an extremely fast dissociation rate but does not bind CD48 or CD59. *Biochemistry.* 33:10149–10160.
44. Cabanas, C., and N. Hogg. 1993. Ligand intercellular adhesion molecule 1 has a necessary role in activation of integrin lymphocyte function associated molecule 1. *Proc. Natl. Acad. Sci. USA.* 90:5838–5842.
45. Lemmon, M.A., J.M. Flanagan, J.F. Hunt, B.D. Adair, B.J. Bormann, C.E. Dempsey, and D.M. Engelman. 1994. Glycophorin A dimerization is driven by specific interactions between transmembrane alpha-helices. *J. Biol. Chem.* 267: 7683–7689.
46. Bormann, B.J., W.J. Knowles, and V.T. Marchesi. 1989. Synthetic peptides mimic the assembly of transmembrane glycoproteins. *J. Biol. Chem.* 264:4033–4037.
47. Rutledge, T., P. Cosson, N. Manolios, J.S. Bonifacino, and R.D. Klausner. 1992. Transmembrane helical interactions: zeta chain dimerization and functional association with the T cell antigen receptor. *EMBO (Eur. Mol. Biol. Organ.) J.* 11: 3245–3254.
48. Jones, E.Y., K. Harlos, M.J. Bottomley, R.C. Robinson, P.C. Driscoll, R.M. Edwards, J.M. Clements, T.J. Dungeon, and D.I. Stuart. 1995. Crystal structure of an integrin-binding fragment of vascular cell adhesion molecule-1 at 1.8 Å resolution. *Nature (Lond.).* 373:539–544.
49. Horton, R.M., H.D. Hunt, S.N. Ho, J.K. Pullen, and L.R. Pease. 1989. Engineering hybrid genes without the use of restriction enzymes: gene splicing by overlap extension. *Gene (Amst.).* 77:61–68.
50. Diamond, M.S., D.E. Staunton, S.D. Marlin, and T.A. Springer. 1991. Binding of the integrin Mac-1 (CD11b/CD18) to the third immunoglobulin-like domain of ICAM-1 (CD54) and its regulation by glycosylation. *Cell.* 65:961–971.
51. van Kooyk, Y., E. van de Wiel-van Kemenade, P. Weder, R.J.F. Huijbens, and C.G. Figdor. 1993. Lymphocyte function–associated antigen 1 dominates very late antigen 4 in binding of activated T cell to endothelium. *J. Exp. Med.* 177: 185–190.
52. Randi, A.M., and N. Hogg. 1994. I domain of beta-2 integrin lymphocyte function-associated antigen-1 contains a binding site for ligand intercellular adhesion molecule-1. *J. Biol. Chem.* 269:12395–12398.
53. Stanley, P., P.A. Bates, J. Harvey, R.I. Bennett, and N. Hogg. 1994. Integrin LFA-1 alpha subunit contains an ICAM-1 binding site in domains V and VI. *EMBO (Eur. Mol. Biol. Organ.) J.* 13:1790–1798.
54. Lee, J.O., P. Rieu, M.A. Arnaout, and R. Liddington. 1995. Crystal structure of the A domain from the alpha subunit of integrin CR3 (CD11b/CD18). *Cell.* 80:631–638.
55. Bajt, M.L., T. Goodman, and S.L. McGuire. 1995. beta 2 (CD18) mutations abolish recognition by I domain integrins LFA-1 (alpha L beta 2, CD11a/CD18) and Mac-1 (alpha M beta 2, CD11b/CD18). *J. Biol. Chem.* 270:94–98.